

A Call to Action

Aid Geostationary Space Situational Awareness with Commercial Telescopes

Capt Daniel Moomey, USAF

Disclaimer: The views and opinions expressed or implied in the *Journal* are those of the authors and should not be construed as carrying the official sanction of the Department of Defense, Air Force, Air Education and Training Command, Air University, or other agencies or departments of the US government. This article may be reproduced in whole or in part without permission. If it is reproduced, the *Air and Space Power Journal* requests a courtesy line.



The accumulation of man-made objects in Earth orbit increases with each space launch. Early in the space age, congestion of the common Earth orbit regions was of little concern, but after more than 50 years of launches, satellites now orbit our planet with closer spacing to one another than ever before. This article addresses this issue, particularly for the geostationary (GEO) orbit region.

The congested, contested, and competitive space domain could have a global impact on people's lives because the likelihood of an on-orbit satellite collision is continually increasing.¹ In addition to civil services' dependence on space-based assets, the US military has become more reliant on them and places a high value on those assets. As space becomes not only more congested but also more contested, the types and numbers of resources required to gain and maintain space situational awareness (SSA) must increase.

Maintaining accurate orbit estimations for all man-made Earth-orbiting objects (also known as resident space objects [RSO]) has become quite difficult because of their steadily growing numbers. The US Air Force created and maintains the satellite catalog, which is also one of the missions for the Joint Space Operations Center (JSpOC), located at Vandenberg AFB, California. To facilitate this mission, the Air Force maintains a global network of radar and optical telescope sites collectively known as the Space Surveillance Network (SSN). This network is primarily responsible for generating and reporting on the locations and trajectories of RSOs to the JSpOC.² Over the decades, the size of the satellite catalog has grown, taxing the resources of the SSN. According to the *Enabling Concepts for Space Situational Awareness* document (2007), “The existing Space Surveillance Network . . . was not designed, and is insufficient, to support Space Control needs (e.g. Inadequate coverage to provide persistent surveillance of threats).”³

The additional demand on sensor tracking resources has become especially true for SSN sensors tasked to track GEO RSOs. New tracking assets have recently come online that can observe dim objects (down to the 21st visual magnitude [vm]).⁴ For example, two separate collection surveys have independently observed a bimodal brightness distribution of objects in and around GEO. Figure 1 depicts this distribution collected during both the 2006 European Space Agency (ESA) Space Debris Survey and the 2010 Air Force Research Laboratory (AFRL) Panoramic Survey Telescope and Rapid Response System (Pan-STARRS or PS1) GEO Survey. Throughout both surveys, observations were taken of objects that traversed the camera's field of view. The detection threshold of the PS1 system drops off at higher vm with higher rates of transit, shown in the dashed, dotted, and solid lines, and is measured in arcseconds per second (as/s).⁵

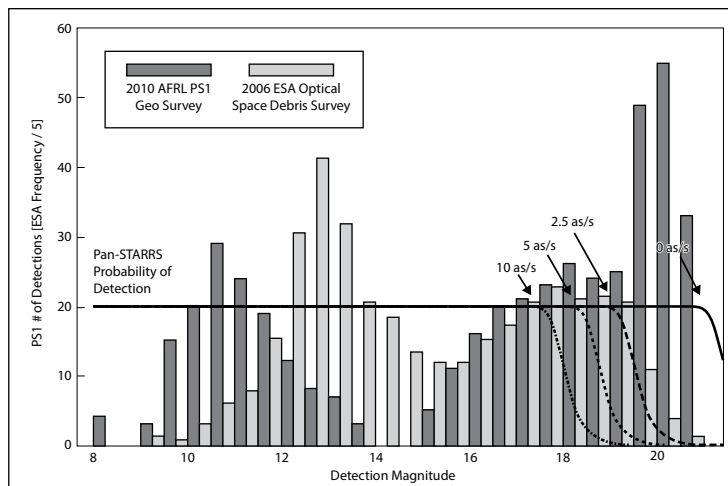


Figure 1. GEO survey brightness histogram. (Reprinted from Mark Bolden, Paul Sydney and Paul Kervin, “Pan-STARRS Status and GEO Observations Results” [paper presented at the Advanced Maui Optical and Space Surveillance (AMOS) Technologies Conference Proceedings, Maui, HI, 2011], [2], “Figure 2: AFRL & ESA Geo Survey Comparison,” http://www.amostech.com/TechnicalPapers/2011/Orbital_Debris/BOLDEN.pdf.)

The figure shows a substantial population density curve of relatively bright and presumably large objects between 8th and 16th vm. In addition, another substantial population of much dimmer objects exists between 15th and 21st vm. This bimodal distribution indicates the existence of a substantial population of presumably small, dim objects not typically observed by the SSN. Although existing operational tracking systems can observe this class of objects, a lack of available sensor time caused by the demands of higher priority taskings has largely prevented the consistent tracking of these objects. Thus, most of them are not regularly maintained as part of the satellite catalog. Without regular orbit maintenance, they cannot be screened for conjunction analysis, leaving an unquantified risk of collision for objects in GEO.⁶

According to *Continuing Kepler's Quest: Assessing Air Force Space Command's Astrodynamics Standards*, "The committee [for the Assessment of the US Air Force's Astrodynamics Standards] believes that the primary limitation in the current system for objects not experiencing significant drag is not the accuracy of the algorithms, but rather the quantity and the quality of the sensor tracking data. The key system limitations are current sensor coverage, understanding of the quality of the observations, and the challenge of fusing disparate data from different systems and phenomenology. Understanding the quality or statistics of the observations is necessary for obtaining a realistic covariance, which is needed for computing an accurate probability of collision."⁷

In an attempt to alleviate the problem of an overburdened SSN and to increase coverage, the Department of Defense has in the past sparingly employed commercial off-the-shelf (COTS) electro-optical telescope systems for space surveillance purposes. Recent technological developments in the design of mounts, optics, and focal planes have produced lower-cost, higher-capability, and higher-accuracy COTS astronomical equipment.⁸ The current operational and fiscal environment has created a greater need to find effective, suitable, and more cost efficient solutions to operational problems. In an attempt to apply these principles to aid the GEO SSA mission, this article considers the following question: *Can a large-scale employment of small-aperture COTS telescopes augment the SSN's observing capacity of the geostationary belt without degrading the quality of orbit estimations?*⁹

The results from the study offer a good indication that COTS equipment could serve the Air Force's mission needs and enable the Department of Defense to reallocate tasking time on the existing larger, more capable optical SSN assets to observe smaller, dimmer, lower-priority objects that have thus far remained largely undetected and/or uncataloged. Such a change should occur in a manner consistent with the committee's remarks (see above) and should follow the principles of SSA:

- integration
- accuracy
- relevance
- timeliness
- fusion
- accessibility and security

- survivability/sustainability/deployability
- unity of effort
- interoperability¹⁰

Perhaps most importantly, achieving such a state would aid the goals and vision of the commander of Air Force Space Command (AFSPC) towards realizing SSA:

1. predictive intelligence of all threats to space-related systems
2. persistent coverage of threats (e.g., no loss of track)
3. timely attribution of attacks/threats
4. integrated SSA, fusion of intelligence, surveillance, reconnaissance, and environmental
5. determination of the adversary's capability, purpose, and intent¹¹

To validate the above, the study used the following method to design and test a system that addresses each of the AFSPC commander's needs. First, a basic systems engineering approach determined an appropriate system specification using optical COTS equipment and software that could reliably observe high-value GEO RSOs to meet the commander's five mission requirements. Next, the author devised a test system to determine the feasibility of applying such a concept to the operational environment. Doing so required the capture, processing, analysis, and comparison of observations from a small optical COTS system with the operational SSN systems. Consequently, the first objective was to determine the accuracy of the satellite metric observations of the test system. Such observations are represented as a series of numerical values such as time, right ascension, and declination. The second objective called for determining the feasibility and quality of performing an orbit determination and differential correction of the observed RSOs by using the most recent published orbit estimations in two-line element (TLE) set format from the JSpOC. Only the observations from the test system were included to perform differential corrections on the TLEs with the intent of including as much angular coverage as possible to increase the orbit determination accuracy.

Using only COTS equipment and commercial or free software, the study demonstrated a method to optically observe high-value GEO RSOs, create high-accuracy metric observations, and use those observations to converge on an update to the JSpOC-published TLE. Additionally, satellite ephemerides were computed and modeled in a Systems Tool Kit simulation for illustrative comparison against the respective TLEs. Having established the accuracy, the study then conducted a performance comparison of metric accuracies between the experimental setup and the current SSN systems.

Assumptions and Limitations

Assumptions for the project as a whole began with an expectation of how the SSA mission will proceed in the future. The study first assumed that the demand for

timely, accurate, and complete SSA capabilities will continue to grow. It also assumed that the primary burden for SSA operational tasking, collection, processing, exploitation, and dissemination will continue to fall to the JSpOC.¹² The center will proceed with development of its Mission System, employing a scalable server architecture and providing additional processing capacity necessary to ingest the observations generated by this study's proposed system for satellite catalog maintenance. In addition, although not invariably true, the study assumed that existing GEO-observing SSN sites are tasked, by and large, with high-priority observation of high-value GEO RSOs, which are typically sizable and relatively bright. This provides the foundation to reduce high-priority taskings for the existing GEO SSA assets.

Consequently, the observations collected were limited to large, bright, geostationary satellites in the visible band, using inexpensive COTS equipment. The number and quality of the collections were affected by the weather, local sky brightness, and limitations of the equipment. The angular accuracy and precision of the observations were also constrained by image processing techniques such as the ability to determine precisely the time at which the observation was created. Synchronizing the computer's clock, which stored the images, with the US Naval Observatory's master clock from the observatory's website established an accurate time of capture. The stated accuracy for the observatory and the National Institute of Standards and Technology time servers is to the nearest whole second (± 0.5 second).¹³

Analysis of the observations utilized general-perturbation TLEs published by the JSpOC for a baseline comparison. When the study used general-perturbations accuracy, the difference between the observed position and the expected position of the satellites was typically within the average accuracy of a JSpOC GEO TLE. Because of this finding and the relatively short time span of the observing periods, the study could not treat the TLEs as a suitable truth reference from which to validate a sensor bias value for the test system.

Because the study was constrained to address the stated goals/vision of the AFSPC commander for the case of the high-value assets along the geostationary belt, the work focused on a single-point design analysis. The analysis sought to optimize the system design by minimizing the diameter of the primary aperture and maximizing the observable ν_m while making reasonable worst-case assumptions about the nature of an RSO and the observing conditions. In constraining the study to concentrate on system design and observation-quality analysis, the author recognizes other principles of SSA—primarily security, deployability, and sustainability—as important, addressing them in the next section but not analyzing them in depth.

Operational System Design and Specifications

According to the AFSPC commander, additional SSA capabilities are required to augment current capacity. From the stated mission need to the derivation of mission requirements, measures of effectiveness, and measures of performance, the study will present a notional system specification and system performance to show how a large-scale implementation of COTS equipment can aid the GEO SSA mission. Here, this implementation is referred to as the Small Aperture Deep Space Surveil-

lance system (SADSS). The requirements shown in table 1 were developed specifically for this study and derived from the AFSPC commander's goals and vision to attain SSA. The mission requirements are intended to address the five goals. From the requirements, measures of effectiveness are derived in table 1 as well. The goals of the measures of effectiveness are to serve as indicators of the system's ability to meet each of the mission requirements. From the measures of effectiveness, design parameters and measures of performance are also established (see table 2). For quantitative values of the measures of performance, refer to the author's original thesis work.¹⁴

Table 1. Mission requirements and measures of effectiveness for SADSS

MR1	System shall be able to create observations with the capability to produce element sets for GEO objects, which are as accurate or more accurate than element sets created using observations from the current SSN (addresses goal 1)
	MOE 1-1 Sensor metrics accuracy
	MOE 1-2 Ephemeris accuracy
MR1	System shall be capable of observing high-value space assets at all longitudes of the geosynchronous belt (addresses goals 1 and 2)
	MOE 2-1 Probability of detection of a high-value GEO RSO
	MOE 2-2 Coverage area
MR3	System shall be capable of providing persistent coverage for targets of interest anywhere along the geosynchronous belt (addresses goal 2)
	MOE 3-1 Coverage time
MR4	System shall be capable of providing near-real-time observations of high-value GEO RSOs to the JSpOC (addresses goal 3)
	MOE 4-1 Observation sample rate
	MOE 4-2 Astrometry plate solution success ratio
MR5	System shall be capable of providing observations in a format ingestible to its customers (addresses goal 4)
	MOE 5 Differential correction from TLE using SADSS observations
MR6	System shall be capable of providing information useful for determining capabilities and purpose of the observed RSOs (addresses goal 5)
	MOE 6 SNR of RSO's point spread function over time

MR = mission requirement
 MOE = measure of effectiveness
 SNR = signal-to-noise ratio

Table 2. SADSS final system specification and measures of performance

MR	MOE & Effect	Design Parameters & Specifications			MOP
MR1	MOE 1-1 High accuracy sensor metrics	Pixel field of view 2 arcsec (12 micrometer pixel pitch)	Precision of image time < ±0.133 sec		MOP 1-1-1
					Sensor sigma
	MOE 1-2 High confidence and accuracy of generated ephemeris	Sun angle limits 0°–100°	Sensor sigma Timing precision + imaging precision = 5 arcsec (est.)		MOP 1-1-2
					Sensor bias
MR2	MOE 2-1 High probability of detection	Aperture diameter 25 cm	RSO area ≥ 4 m ²	Band avg. CCD QE 75%	MOP 2-1-1
	MOE 2-1 High probability of detection	CCD Noise Read 8 e-/pix Dark .2 e-/pix/sec		Sky noise Diego Garcia + 2vm/arcsec ²	MOP 2-1-2
	MOE 2-2 Large coverage area	Focal length 1.25 m	Film format 30.5 x 30.5 mm		Detected signal
MR3	MOE 3-1 Coverage time	Sun angle limits 0°–100°	Number of sites 5		MOP 2-2-1
					Observed orbit
					MOP 3-2-2
MR4	MOE 4-1 Increased observation rate	Exposure time 1 sec	Processing time < 6.5 sec		Minimum elevation
	MOE 4-2 High astrometry solution ratio	FOV 2 ^{o2} (1.4°x1.4°)	Aperture diameter 25 cm		MOP 4-1
	MOE 4-2 High astrometry solution ratio	Focal length 1.25 m	Aperture diameter 25 cm		Exposure time + Processing time
MR5	MOE 5 Successful differential correction	Calibrated data Requires validation	Compatible message GEOSC format		MOP 4-2-1
					no. of stars detected
MR6	MOE 6 Actionable information	SNR sample rate Observation sample rate	SNR error Requires customer input		MOP 4-2-2
					Image distortion
MR5	MOE 5 Successful differential correction	Calibrated data Requires validation	Compatible message GEOSC format		MOP 5
					Residual rejection %
MR6	MOE 6 Actionable information	SNR sample rate Observation sample rate	SNR error Requires customer input		MOP 6
					Quality of light curve metrics

MR = mission requirement
 MOE = measure of effectiveness
 MOP = measure of performance
 arsec = arcseconds
 vm = visual magnitude
 CCD = charge coupled device
 FOV = field of view
 SNR = signal-to-noise ratio
 QE = quantum efficiency
 GEOSC = geoscience
 RMS = root mean square

From the mission requirements, two fundamental differences emerge between previous efforts to incorporate small-aperture COTS solutions and the work presented here. From MR2, the proposed system would be charged with observing only high-value GEO RSOs. According to Mark Bolden, Paul Sydney, and Paul Kervin, “It has been theorized and widely accepted that the bright object population (< 16th VM) is dominated by artificial satellites both active and inactive, while the faint object population is composed mostly of debris.”¹⁵ Thus, the study assumed that high-value GEO RSOs, by and large, are brighter than 16th vm. MR3 also differs from that in previous studies since it requires persistent coverage of an RSO. To address this requirement, the study configured the sensors to employ rate tracking of a particular longitudinal band of the GEO belt. Rate tracking affords several advantages, such as an increased probability to detect an RSO during partly cloudy sky conditions; furthermore, it offers the capability to perform sustained-event monitoring during hours of darkness on RSOs of interest. Current optical SSN sensors can observe in rate-track mode but typically operate in sidereal mode in an effort to expand the coverage area with the limited number of telescopes.¹⁶ As a result, existing SSN systems observe each satellite for only seconds per day.

Perpetual rate tracking fulfills MR3 in providing persistence, but it carries a fundamental trade. That is, the surveillance area of the system is static with relation to the GEO belt, leaving the rest of the sky unsurveilled. To overcome this deficiency, one must supply the system as a whole with multiple sensors at multiple sites, each observing a different portion of the belt and spanning its entirety (fig. 2). The total proposed system architecture would employ an array of approximately 60 telescopes at each of the five sites. The list of locations includes the three Ground-Based Electro-Optical Deep Space Surveillance (GEODSS) locations (Maui, Hawaii [1]; Socorro, New Mexico [2]; and Diego Garcia [3]), as well as the planned space surveillance telescope site in Exmouth, Australia (4), and, finally, an additional array on Ascension Island (5). The five locations shown in figure 2 with numbered coverage fans were chosen to address system sustainability and deployability considerations in terms of security, maintenance personnel, and common communications architecture—already established at each of the proposed sites.



Figure 2. Notional sensor coverage for the SADSS network at 33° elevation

From the specifications above, the study chose a design using a Takahashi CCA250 astrograph (\$17,000 each) paired with an e2V CCD230-42 camera (\$42,000 each) as a reference that meets the system specifications. With mounting and housing costs combined with the equipment, the price per site for 60 sensors totals approximately \$3.5 million before installation. By comparison, the GEODSS telescopes cost \$3.3 million per site in fiscal year 2000.¹⁷ Therefore, as a rough order of magnitude, acquisition of the two systems is estimated at near cost parity.

Method

Several analyses determined the selection of the system outlined above. First, an analysis of satellite brightness as a function of size, reflectivity, and lighting angle would establish conditions that would yield a 16th vm signal to the observer. To determine a single value for reflectance of a high-value RSO, the study used the reflectance value for multilayered insulation satellite coating. Heather Rodriguez and her colleagues performed a spectral analysis to determine the optical properties of multilayered insulation. Figure 3 shows the reflectance band in the visible spectrum for the insulation sampled.¹⁸ The study assumed a value of 15 percent reflectance and chose a maximum lighting angle (beta angle) of 100° so the system could offer at least 8 hours of continuous track time per night for the purpose of tracking a sufficient orbit length to create highly accurate orbit estimations.¹⁹

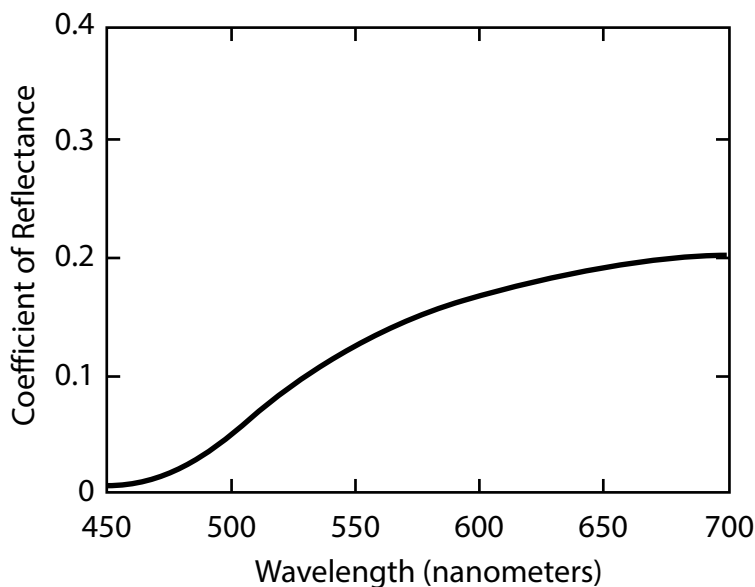


Figure 3. Reflectance of copper-colored Kapton multilayered insulation. (From Heather Rodriguez et al., “Optical Properties of Multi-Layered Insulation” [paper presented at the AMOS Conference Proceedings, Maui, HI, 2007], “fig. 9,” [page 9], <http://www.amostech.com/TechnicalPapers/2007/Poster/Rodriguez.pdf>.)

Next, the study computed the contribution of atmospheric attenuation as a function of elevation angle.²⁰ From this finding, a reasonable worst-case observing scenario was chosen—specifically, from the Diego Garcia GEODSS site with a minimum viewing angle of 33° elevation with a gibbous moon 45° from the sight line. Though the GEODSS sensors were designed to perform at elevation angles as low as 20° , for the chosen SADSS sites, full global coverage of the GEO belt occurs with a minimum of 33° elevation. With these reasonable worst-case conditions and constraints defined, the study applied radiometric equations to determine that an RSO of four square meters (4 m^2) could be observed at 16th vm (fig. 4).²¹

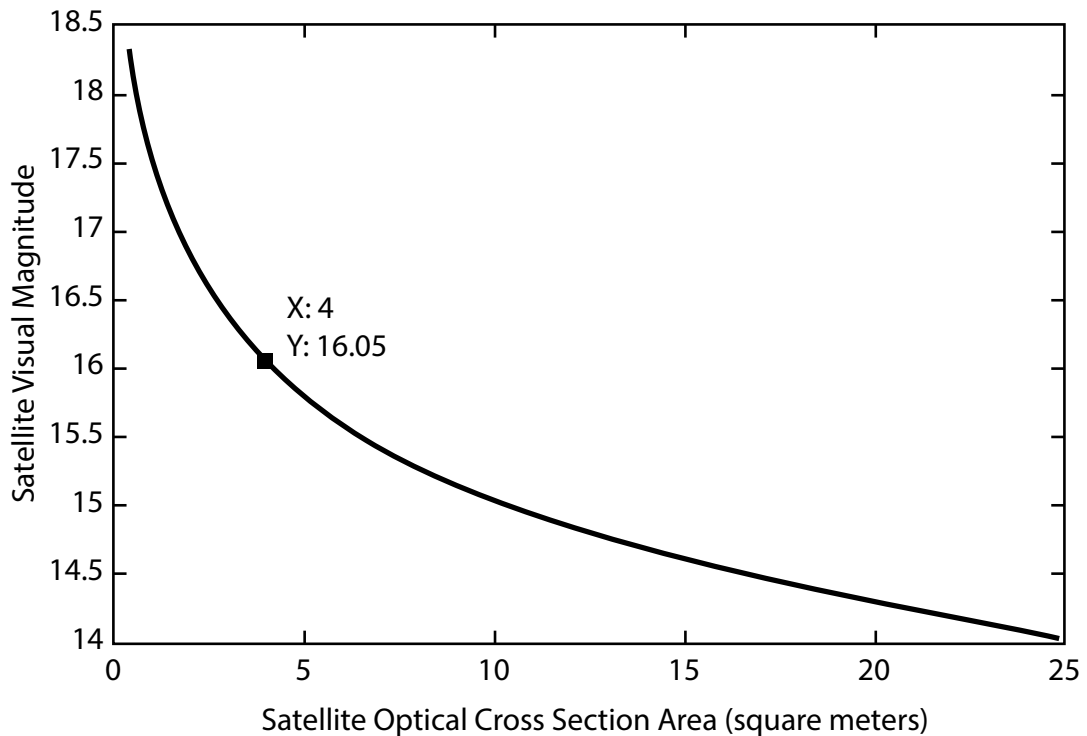
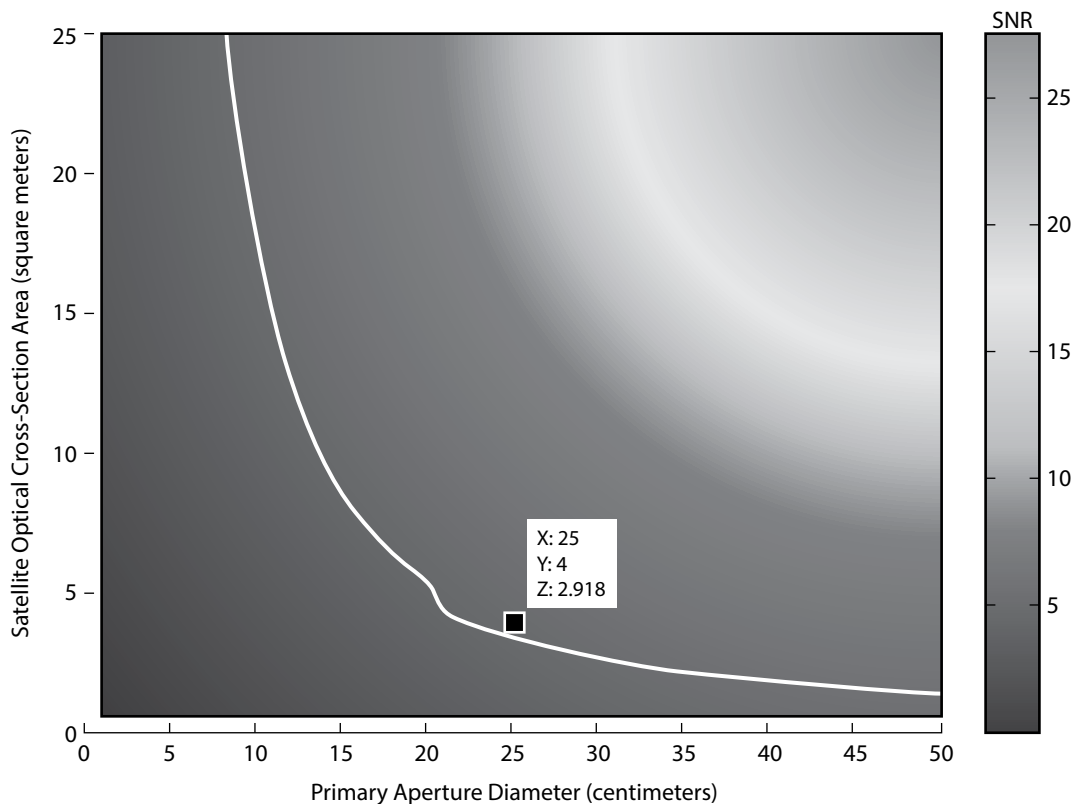


Figure 4. Satellite visual magnitude versus surface area at 100° sun angle

To determine the percentage of GEO satellites that a 4 m^2 detection threshold corresponds to, the study generated a list of GEO RSOs from Space-Track.org and used the McCants radar-cross-section satellite list to cross-reference for radar-cross-section values.²² The cross-referenced list identified 77 percent of the RSOs to be $\geq 4 \text{ m}^2$ radar cross section.

After applying assumptions and constraints to radiometric equations, the study completed its analysis of the trade space between detectable surface area and primary aperture diameter. The result is shown in figure 5, where the white isoline represents a signal to noise ratio of 2.5—chosen as the minimum threshold for

detection.²³ For apertures of 20 centimeters (cm) and below, the study assumed a refracting instrument and, for above 20 cm aperture, applied a reflecting telescope with a 30 percent obscuration, which accounts for the horizontal shift in the line at the 21 cm aperture value. Figure 5 predicts a necessary aperture of 22 cm for detecting a 4 m² object. With the common availability of 25 cm COTS optical designs and the margin of performance offered from the reasonable worst-case imaging scenario, the study chose a 25 cm optic. The predicted detection threshold with a 25 cm aperture for a 4 m² RSO yields a signal to noise ratio of 2.9. Although the system is designed to track a 4 m² object, it is possible to track smaller objects by using a more restrictive sun angle. The maximum angle profile for a 2 m² object using a SADSS sensor is estimated to be 81°, still allowing for an annual average of seven hours of track time per night.



SNR = signal-to-noise ratio

Figure 5. RSO surface area versus primary aperture at 100° sun angle

With the system specifications determined and parts selected, the next step involved testing the equipment in an operationally relevant environment. Unfortunately, the institute did not have SADSS-comparable equipment on hand with which to validate its performance. Instead, the existing Air Force Institute of Technology

TeleTrak network of telescopes and computer-control equipment was used to collect the sample observations. The telescope chosen was an Orion 80 mm short tube with a .5 focal reducer / field flattener mated to an Astrovid Stellacam II camera on a Meade LX200GPS mount. Table 3 outlines the difference between the SADSS-proposed sensor and the test article equipment.

Table 3. Differences between SADSS and TeleTrak test equipment

	<i>Cost</i>	<i>Aperture</i>	<i>Sample rate</i>	<i>FOV</i>	<i>IFOV</i>	<i>Time precision</i>	<i>Sigma in RA</i>
SADSS	\$70K	25 cm	7.5 sec	1.4° x 1.4°	2.5 arcsec	< ± 0.133 sec	5 arcsec (est.)
TeleTrak	\$500	8 cm	1.07 sec	1.2° x 1.6°	5.6 arcsec	± 0.5 sec	11 arcsec

FOV = field of view

IFOV = instantaneous field of view

RA = right ascension

The field of view produced by the optical camera assembly is approximately 1.2° x 1.6° with an angular pixel resolution of 5.6 arcseconds/pixel. This field of view was chosen deliberately to ensure that the images would contain a sufficient number of bright reference stars for the software algorithms to accurately and repeatedly produce results for the location of RSOs relative to the inertial reference frame provided by the background stars—a process known as astrometry. From the astrometry-corrected images, topocentric right ascension and declination angles of detected RSOs are measured by using the highly precise positions of known background stars in the captured images. From these observations, one can perform an orbit determination.

First, a highly accurate star catalog is needed for a baseline reference to the celestial sphere. The stars in the image must then be identified by comparing their positions and relative intensities to each other and then comparing the orientation pattern to the known star catalog for a match. When the telescope is tracking in sidereal mode, the stars in the image can be chosen judiciously to make this identification simpler. However, in rate-tracking mode, the star field is continuously changing, and the use of star-matching software, such as that provided by *astrometry.net*, can be highly advantageous to aid in processing large data sets with unknown star fields.²⁴ Once the star field is identified, multiple coordinate transformations must then take place to create an observation in an Earth-centric inertial reference frame, which then allows it to be applied for orbit-determination purposes.

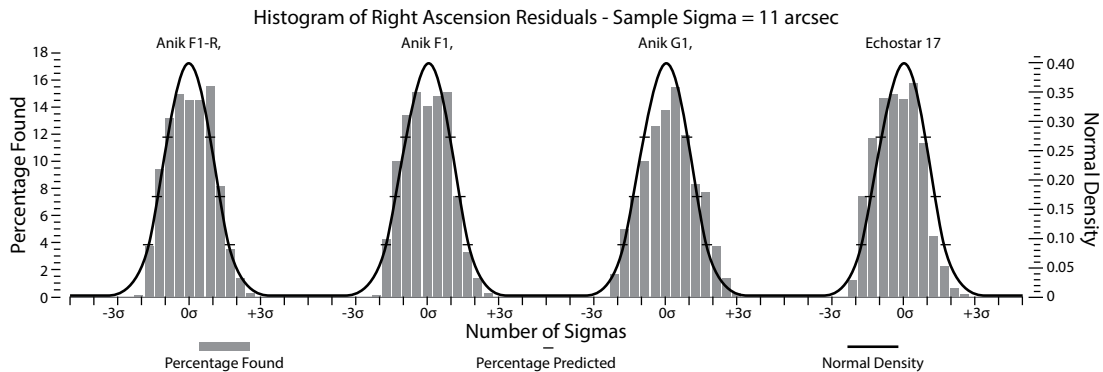
Maintenance of interoperability and compliance with the SSN's standard message format for optical observations, known as a B3 report, require transformation of the topocentric right ascension and declination angular measurements into a South-East-Zenith right-handed orthogonal coordinate system. The angular measurements from this coordinate system are reported as azimuth and elevation angles centered on the observing sensor's location—shown in Vallado's Algorithm 28.²⁵ Operationally, the JSpOC receives the metric observation report in the sensor's local azimuth and elevation reference frame. These angles are then transformed to an Earth Centered Inertial reference frame. Once in the frame, the most recent TLE for the RSO is applied for comparison with the measurements, and the initial residuals are generated.

From there, the Simplified General Perturbations version 4 (SGP4) algorithm used by AFSPC to differentially correct orbit estimations can be executed, using the new measurements to create an updated TLE. For the research herein, the majority of these steps applied. However, Analytical Graphics Incorporated's Orbit Determination Tool Kit software allows for ingestion of the ground-based right ascension and declination observations in the topocentric reference frame directly with knowledge of the observing site's location. Doing so eliminated the need to manually apply Vallado's algorithms to the observations, thus decreasing the complexity of the processing chain.

In gathering the observations for processing and orbit determination, the study used two observing campaigns. The first, which took place from 26 October 2014, determined the sensor precision, and the second, which occurred over three consecutive nights spanning 16–18 January 2015, was used to perform orbit-determination comparison with JSpOC TLEs. The observing target was the *Anik F1* cluster, located at an elevation of 38° in the southwest portion of the sky from Dayton, Ohio. The cluster consists of the *Anik F1*, *Anik F1-R*, and *Anik G1* satellites. *Echostar 17* leads the Anik cluster by 0.2° in right ascension and was also observed in the field of view. All four of these satellites are relatively large communications satellites.

Results

From the 26 October 2014 data set, the study determined sensor precision values in both the right ascension and declination components for each of the four satellites across all 17,000 valid observations extracted from the 19,000 images (figs. 6 and 7). The right ascension sigma (fig. 6) indicates a secondary systemic error which is presumed to be primarily caused by timing.



arcsec = arcseconds

Figure 6. Sigma histogram of right ascension residuals from 26 October 2014

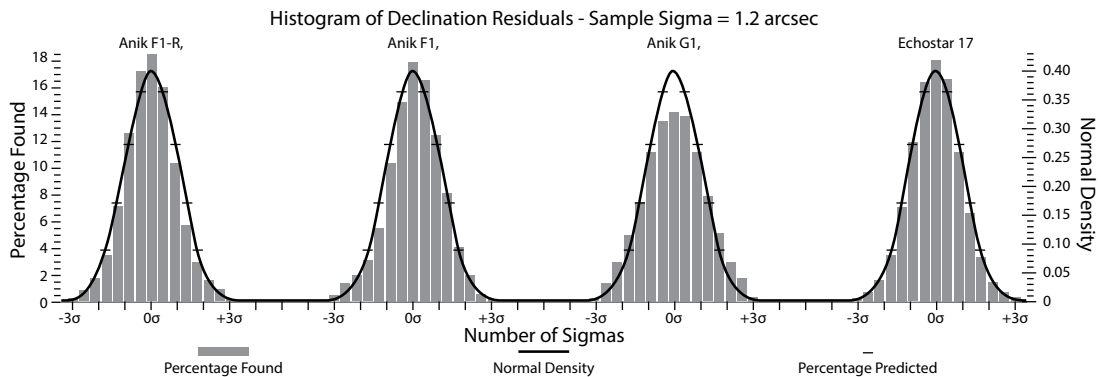


Figure 7. Sigma histogram of declination residuals from 26 October 2014

From the January observing campaign, the ephemeris generated from the 8,000 observations sampled once per 10 seconds shows good correlation to the corresponding JSpOC TLEs. In performing the differential corrections, the study showed that all four of the tracked RSOs converged on a solution directly from the JSpOC's most recently published TLE. Each least squares orbit determination run was initialized using the JSpOC TLE, and each came to a convergence with close resemblance to the TLE. A comparison between the initial TLE and the least squares solution from the TeleTrak observations is shown in table 4. Figures 8 and 9 depict the relative change in position over 24 hours between the generated ephemeris from the test data (EPH) and the JSpOC published TLE. The differential drift rate was reduced by an order of magnitude over test case 2, which saw a difference of about 10 kilometers in semimajor axis between the TLE and the ephemeris. Figure 10 shows how the propagation error grows over the two days after the last observation on the untracked, daylight side of the orbit. The viewing perspective for the following figures was set to a few hundred kilometers above the GEO belt and centered between *Echostar 17* and the Anik cluster. Thus, the relative size of the JSpOC GEO TLE error ellipsoid in figures 8 and 9 is greatly exaggerated with respect to Earth.

Table 4. Ephemeris and TLE comparison from January 2015

SATNO	Source	Epoch	Semimajor axis	Eccentricity	Inclination°	RAAN°	Arg. of Per.°	Arg. of Lat.°
Anik F1 26624	EPH	16:56:28.395	42166.568 km	0.000341	0.09945	85.22445	100.942810	176.29852
	TLE	16:56:28.395	42165.510 km	0.000083	0.10455	88.00984	180.45842	173.45326
Anik F1R 28868	EPH	16:08:05.930	42166.947 km	0.000207	0.08719	62.59837	201.86272	186.73179
	TLE	16:08:05.930	42165.673 km	0.000276	0.09258	70.54715	266.02396	178.74061
Echostar 17 38551	EPH	09:05:20.377	42164.987 km	0.000295	0.09836	77.39478	185.73116	66.11604
	TLE	09:05:20.377	42165.708 km	0.000253	0.10981	19.17635	201.20691	64.34500
Anik G1 39127	EPH	16:16:29.058	42165.067 km	0.000211	0.09797	75.94122	242.24602	175.41940
	TLE	16:16:29.058	42165.427 km	0.000332	0.07944	75.28374	217.96316	176.11927

SATNO = satellite number
 RAAN = right ascension of the ascending node
 Arg. of Per. = Argument of Perigee
 Arg. of Lat. = Argument of Latitude

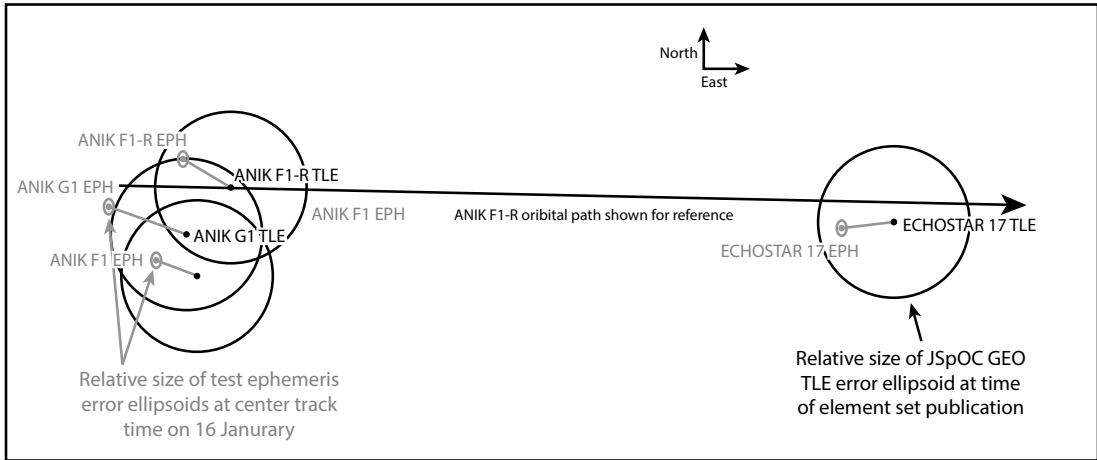


Figure 8. TLE versus ephemeris at center track time on 16 January 2015

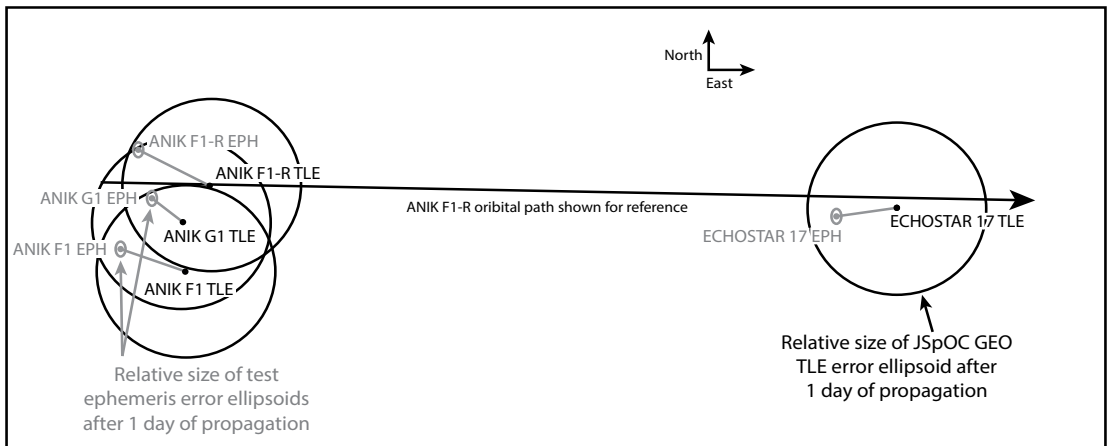


Figure 9. TLE versus ephemeris at center track time on 17 January 2015

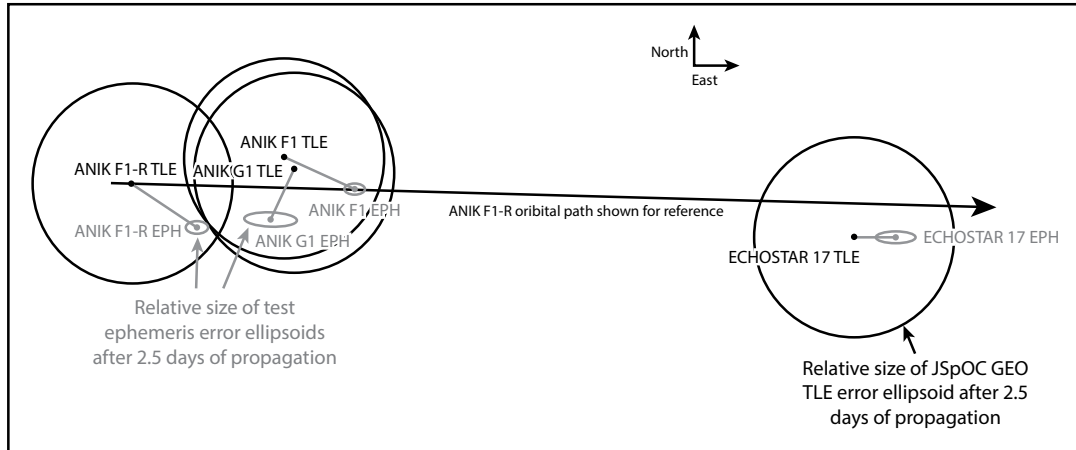


Figure 10. TLE versus ephemeris after 2.5 days of propagation

These test cases produced a proof of concept capable of processing observations from the COTS hardware using only COTS software semiautonomously. In doing so, the JSpOC TLEs were effectively re-created to the average accuracy limits of GEO TLE with only two or three nights of observations. The potential for improvement by performing a similar study over a month's worth of tracking is encouraging. Because of the relatively low fidelity of the TLEs and the lack of transparency of the Analytical Graphics Incorporated special perturbations orbit-determination algorithm and the way it compares to SGP4, though, the causality of the delta between the TLE and the element set created from the test data remains unknown but is probably a mixture of timing accuracy and algorithm mismatch. However, if the SADSS program were to come to fruition, a more comprehensive operational test could be conducted using the current operational algorithms to reduce the unknown errors and come to a more thorough understanding of system performance and its capacity to off-load tasking from the existing optical SSN sensors.

Given the presumption that each object requires an epoch update every 24 hours and that GEODSS is tasked to collect the observations in its normal operational mode, a metric for the GEODSS sensor off-load time can be generated. Assuming an even load across all 9 GEODSS telescopes tracking the 556 SADSS observable satellites, this equates to an average tasking off-load rate of 62 taskings per telescope, requiring 248 observations per night. With a peak generation rate of 116 observations per hour, 2 hours of track time for each telescope could be made free—or 18 observing hours per night of reduced tasking for the GEODSS system as a whole. Given 300 SADSS sensors, each with a 1.4° field of view in rate track mode (15° per hour) and tracking an annual average of 10.5 hours per 24-hour period, the total SSA surveillance rate could be increased by 2,750 degrees squared per hour while also offering much higher persistence for precision orbit determination and event monitoring at a comparable equipment dollar cost to GEODSS.²⁶

Conclusions and Future Work

In an attempt to address the AFSPC commander's visions and goals for achieving SSA in the scope of the GEO case, this study developed and tested a system specification to show performance that could observe spherical, low-reflectance GEO RSOs as small as 2 m² at an 81° beta angle and 4 m² objects out to a 100° beta angle. From a much less capable test system, the study created a method to semiautonomously generate right ascension and declination metric observations. The observation accuracies were found to be 11 to 17 arcseconds in right ascension and 1.2 to 2 arcseconds in declination.

From three nights of TeleTrak observations, element sets were differentially corrected directly from the JSpOC's published TLEs. The corrected orbit estimations had an in-track median covariance of 570 meters at the time of publication and a median vector magnitude with respect to the TLE that was roughly equal to the average accuracy limits of a GEO TLE while utilizing only 5–10 percent of the time span typically used by the JSpOC to generate its GEO TLEs.

Although this result is encouraging, fully answering the research question of *whether a large-scale employment of small-aperture COTS telescopes can augment the SSN's observing capacity of the geostationary belt without degrading the quality of orbit estimations* requires further study. An attempt should also be made to validate the sensor sigma and bias values using the operational sensor calibration processes through the AFSPC A2/3/6SZ office. A SADSS system requirement of 0.133-second timing precision requires at least a factor of four improvement. Ultimately, though, collecting observations from a SADSS-like sensor from one or more of the proposed Department of Defense sites over an entire lunar or maneuver cycle is desirable.

More in-depth trade analysis of the mission needs is also desirable. Such an analysis could address a variety of existing COTS hardware components, mixing and matching parts to find a more optimal solution to satisfy the established requirements. Furthermore, by examining the design over varying observing conditions such as elevation and RSOs known to inhabit a particular sensor field of view, a multipoint design analysis could help to further minimize the cost of the network by employing lower-cost systems along more favorable sight lines.

The overall program cost also needs further investigation and refinement. Provided here was a simple, rough order of magnitude cost for most of the equipment, neglecting installation, computer processing, and operation and maintenance expenses. With a refined program acquisition and sustainment cost, alternative analysis could then determine if building a SADSS network is the best choice for the funds allocated to AFSPC to carry out the GEO SSA mission.

If the Air Force is to formally acquire the system proposed here, then other considerations not discussed within the scope of this effort must be addressed. Such considerations include funding, development, and developmental and operational testing of the system to verify and validate its performance against the system requirements. The developing System Program Office, the Air Force Operational Test and Evaluation Center, and/or the 17th Test Squadron would likely perform these actions, once tasked by AFSPC. To ensure that the data ingested into the SSA mission could be trusted, the AFSPC A2/3/6ZS number validation office would need to

actively monitor sensor calibration, as occurs with all other SSN sensors. The other logistical considerations, such as security, communications, and maintenance plans previously discussed, are also prerequisite to operationalization of the system. However, it is presumed that the risk of these issues would have been partially mitigated by co-locating the SADSS sensors with other actively operated government optical systems. Still, a more in-depth analysis of these considerations should occur prior to moving forward to acquire the system.

Regardless of the chosen solution, the Air Force needs to solve the problem of SSA in order to create and maintain an accurate common operating picture for space. As the mission requirements for achieving and maintaining SSA continue to grow, so will the resource demands to conduct the mission. The questions then become, What is being done now, and what needs to be done to address the needs of today and the problems of tomorrow? 🌟

Notes

1. Patrick J. Payte, "Orbit Determination and Prediction for Uncorrelated Target Detection and Tracking" (MS thesis, Department of Aeronautics and Astronautics, Air Force Institute of Technology [AFIT], Wright-Patterson AFB, OH, 2008); Christine M. Schudrowitz, "The Effects of Observations and Maneuvers on Orbit Solutions" (MS thesis, Department of Aeronautics and Astronautics, AFIT, Wright-Patterson AFB, OH, 2012); and Committee for the Assessment of the US Air Force's Astrodynamics Standards, *Continuing Kepler's Quest: Assessing Air Force Space Command's Astrodynamics Standards* (Washington, DC: National Academies Press, 2012).
2. Headquarters Air Force Space Command / Space Situational Awareness, Command and Control Operations, and Integration Branch (A3C), *Enabling Concept for Space Situational Awareness (SSA)* (Peterson AFB, CO: Headquarters Air Force Space Command/A3C, October 2007).
3. *Ibid.*, 8. See also Payte, "Orbit Determination and Prediction."
4. The apparent visual magnitude (vm) scale is such that the higher the value, the dimmer the object. Each integer increase in order, such as first to second vm, is a decrease in visual brightness by a factor of two-and-a-half. For more information, see "The Astronomical Magnitude Scale," *International Comet Quarterly*, accessed 17 September 2015, <http://www.icq.eps.harvard.edu/MagScale.html>.
5. Mark Bolden, Paul Sydney and Paul Kervin, "Pan-STARRS Status and GEO Observations Results" (paper presented at the Advanced Maui Optical and Space Surveillance Technologies [AMOS] Conference Proceedings, Maui, HI, 2011), http://www.amostech.com/TechnicalPapers/2011/Orbital_Debris/BOLDEN.pdf.
6. Committee for the Assessment of the US Air Force's Astrodynamics Standards, *Continuing Kepler's Quest*, 18; and Bolden, Sydney, and Kervin, "Pan-STARRS Status."
7. Committee for the Assessment of the US Air Force's Astrodynamics Standards, *Continuing Kepler's Quest*, 2-3.
8. Anthony D. Gleckler and Michael C. Butterfield, "Viral Space Situational Awareness" (paper presented at the AMOS Conference Proceedings, Maui, HI, 2012), http://www.amostech.com/TechnicalPapers/2012/Data_Services/GLECKLER.pdf.
9. Daniel Moomey, "Aiding Geostationary Space Situational Awareness Using Small Aperture Commercial Telescopes" (MS thesis, Department of Aeronautics and Astronautics, AFIT, Wright-Patterson AFB, OH, 2015), 3.
10. Headquarters Air Force Space Command/A3CD, *Enabling Concept*, 12, 22-24.
11. *Ibid.*, 14.
12. *Ibid.*, 10.
13. "US Naval Observatory Master Clock," US Naval Observatory, accessed 30 July 2014, <http://tycho.usno.navy.mil/what.html>; and "NIST Internet Time Service (ITS)," National Institute of Standards and Technology, US Department of Commerce, accessed 30 July 2014, <http://www.nist.gov/pml/div688/grp40/its.cfm>.
14. Moomey, "Aiding Geostationary Space Situational Awareness."
15. Bolden, Sydney, and Kervin, "Pan-STARRS Status," [1].

16. Walter J. Faccenda, "GEODSS: Past and Future Improvements," MITRE Corporation, 2000, https://www.mitre.org/sites/default/files/pdf/geodss_faccenda.pdf.
17. A. Thompson, "A GEODSS Sourcebook," 19 October 2008, <http://www.fas.org/spp/military/program/track/geodss.pdf>.
18. Heather Rodriguez et al., "Optical Properties of Multi-Layered Insulation" (paper presented at the AMOS Conference Proceedings, Maui, HI, 2007), <http://www.amostech.com/TechnicalPapers/2007/Poster/Rodriguez.pdf>.
19. Joshua T. Horwood, Aubrey B. Poore, and Kyle T. Alfriend, "Orbit Determination and Data Fusion in GEO" (paper presented at the AMOS Conference Proceedings, Maui, HI, 2011), <http://www.amostech.com/TechnicalPapers/2011/Astrodynamics/HORWOorbitdetermination.pdf>.
20. Carolin Früh and Moriba K. Jah, "Detection Probability of Earth Orbiting Objects Using Optical Sensors," *Advances in Astronomical Sciences* 150 (2014): 13; W. Jody Mandeville et al., "Sky Brightness Analysis Using a Million Ground-Based Electro-Optical Deep Space Surveillance (GEODSS) Observations" (paper presented at the AMOS Conference Proceedings, Maui, HI, 2012), <http://www.amostech.com/TechnicalPapers/2012/POSTER/MANDEVILLE.pdf>; and Kevin Krisciunas and Bradley E. Schaefer, "A Model of the Brightness of Moonlight," *Astronomical Society of the Pacific*, no. 103 (1991): 1033–39.
21. Früh and Jah, "Detection Probability"; Steve B. Howell, *The Handbook of CCD Astronomy*, 2nd ed. (Cambridge, UK: Cambridge University Press, 2006), 73; and Ryan D. Coder and Marcus J. Holzinger, "Sizing of a Raven-Class Telescope Using Performance Sensitivities" (paper presented at the AMOS Conference Proceedings, Maui, HI, 2013), http://www.amostech.com/TechnicalPapers/2013/Optical_Systems/CorbitdeterminationER.pdf.
22. JFCC SPACE/J3, "Space-Track.org," Air Force Space Command, 28 January 2015, <https://www.space-track.org/#/queryBuilder>; and Mike McCants, "Mike McCants' Satellite Tracking Web Pages," 5 September 2014, <https://www.prismnet.com/~mmccants/programs/qsmag.zip>.
23. Früh and Jah, "Detection Probability."
24. "Astrometry.net," US National Science Foundation, US National Aeronautics and Space Administration, and the Canadian National Science and Engineering Research Council, 2015, <http://www.astrometry.net/>.
25. David Anthony Vallado and Wayne D. McClain, *Fundamentals of Astrodynamics and Applications*, 4th ed. (El Segundo, CA: Microcosm Press, Kluwer Academic Publishers, 2013), 272.
26. Robert F. Bruck and Capt Robert H. Copley, USAF, "GEODSS Present Configuration and Potential" (paper presented at the AMOS Conference Proceedings, Maui, HI, 2014), <http://www.amostech.com/TechnicalPapers/2014/Poster/BRUCK.pdf>; and Thompson, "A GEODSS Sourcebook."



Capt Daniel Moomey, USAF

Captain Moomey (BA, University of Toledo; MS, Air Force Institute of Technology) serves on active duty in the United States Air Force. He is a flight commander for the 17th Test Squadron at Schriever AFB, Colorado, overseeing operational testing and evaluation of US Air Force space systems. His previous assignments include a one-year tour overseas to Thule, Greenland, as a crew commander for the 12th Space Warning Squadron where he performed space surveillance and missile warning duties. Captain Moomey served as the space battle manager and operations liaison to the Unified Space Vault at the Joint Space Operations Center, performing space situational awareness duties. He was selected to rebuild, reinstate, instruct, and administrate Air Education and Training Command's space surveillance training course for the 533rd Training Squadron at Vandenberg AFB, California. He then was competitively selected to attend the Air Force Institute of Technology at Wright-Patterson AFB, Ohio, where he completed an MS degree in space systems. Captain Moomey is coauthor of "Revisiting the Chlorine Abundance in Diffuse Interstellar Clouds from Measurements with the Copernicus Satellite," *Astrophysical Journal* 744, no. 2 (January 2012): 1–7.

Let us know what you think!
Leave a comment!

Distribution A: Approved for public release;
distribution unlimited.

<http://www.airpower.au.af.mil>